Magnetic, thermal, and transport properties of layered arsenides $BaRu_2As_2$ and $SrRu_2As_2$

R. Nath, Yogesh Singh, and D. C. Johnston
Ames Laboratory and Department of Physics and Astronomy, Iowa State University, Ames, Iowa 50011, USA
(Received 28 January 2009; revised manuscript received 8 April 2009; published 8 May 2009)

The magnetic, thermal, and transport properties of polycrystalline $BaRu_2As_2$ and $SrRu_2As_2$ samples with the $ThCr_2Si_2$ structure were investigated by means of magnetic susceptibility $\chi(T)$, electrical resistivity $\rho(T)$, and heat capacity $C_p(T)$ measurements. The temperature (T) dependence of ρ indicates metallic character for both compounds with residual resistivity ratios $\rho(310\ \mathrm{K})/\rho(2\ \mathrm{K})$ of 17 and 5 for the Ba and Sr compounds, respectively. The $C_p(T)$ results reveal a low-T Sommerfeld coefficient $\gamma=4.9(1)$ and 4.1(1) mJ/mol K^2 and Debye temperature $\Theta_D=271(7)$ and 271(4) K for the Ba and Sr compounds, respectively. The $\chi(T)$ was found to be diamagnetic with a small absolute value for both compounds. No transitions were found for $BaRu_2As_2$ above 1.8 K. The $\chi(T)$ data for $SrRu_2As_2$ exhibit a cusp at ~200 K, possibly an indication of a structural and/or magnetic transition. We discuss the properties of $BaRu_2As_2$ and $SrRu_2As_2$ in the context of other $ThCr_2Si_2$-type and ZrCuSiAs-type transition metal pnictides.

DOI: 10.1103/PhysRevB.79.174513 PACS number(s): 74.70.−b, 75.40.Cx, 65.40.Ba

I. INTRODUCTION

The recent discovery of superconductivity in the layered oxypnictide compound $LaFeAsO_{1-x}F_x$ with superconducting transition temperature $T_c=26$ K has generated great excitement.[1] Subsequently a series of compounds $LnFeAsO_{1-x}F_x$ (e.g., Ln=Ce, Nd, and Sm) (abbreviated as 1111) have been reported with T_c ranging from 10 to 55 K,[2–5] where the high T_c of 55 K was reached for $SmFeAsO_{1-x}F_x$.[2] All these compounds crystallize in a tetragonal unit cell of ZrCuSiAs structure type.[6] Later on another series of compounds $A_{1-x}K_xFe_2As_2$ (A=Ba, Sr, Ca, and Eu) (122) (Refs. 7–11) with the tetragonal $ThCr_2Si_2$ structure type[12] was discovered where the maximum T_c achieved was 38 K.

A common feature of both 1111 and 122 compounds is the identical FeAs layers separated by the LnO or A layers perpendicular to the crystallographic c-axis. Undoped metallic parent compounds of both types show a spin-density wave (SDW) which coexists with a distorted structure at temperatures $T \lesssim 200$ K.[4,13–20] Superconductivity in both series is sometimes assumed to be intimately connected with the SDW anomaly in the FeAs layers.[7,13] Electron or hole doping suppresses both the SDW and structural transition and facilitates the superconductivity. However, it is still unresolved whether the structural transition and/or the magnetism associated with the SDW play a vital role for the occurrence of superconductivity. There exist a few 122 compounds $BaNi_2P_2$,[21] $BaNi_2As_2$,[22] $LaRu_2P_2$,[23] $CsFe_2As_2$, and KFe_2As_2,[10] where even the undoped compound itself shows superconductivity at low temperatures. It is of interest to look for further new systems with different transition metal ions where one can try to achieve an enhanced T_c.

Motivated by the above progress, we turned our attention toward Ru-based layered compounds. So far in the Ru series, $LaRu_2P_2$ which has the $ThCr_2Si_2$-type structure is known to have $T_c=4.1$ K.[23] $BaRu_2As_2$ and $SrRu_2As_2$ compounds also crystallize in the body-centered-tetragonal $ThCr_2Si_2$ structure with space group $I4/mmm$. The reported lattice constants are ($a=4.152$ Å, $c=12.238$ Å) and ($a=4.168$ Å, $c=11.179$ Å) for the Ba and Sr compounds, respectively.[23,24] As shown in Fig. 1, Ru atoms in a square lattice are coordinated by As to form infinite RuAs layers and the layers are separated by Ba layers, similar to the AFe_2As_2 compounds. Because $BaRu_2As_2$ and $SrRu_2As_2$ are isoelectronic to the above undoped AFe_2As_2 compounds, a comparison of the properties of these two series of compounds is of great interest. A detailed investigation of the physical properties of the Ru compounds has not been reported yet. Herein we report a detailed characterization of polycrystalline $BaRu_2As_2$ and $SrRu_2As_2$ by means of magnetic susceptibility $\chi(T)$, electrical resistivity $\rho(T)$, and heat capacity $C_p(T)$ measurements. We will

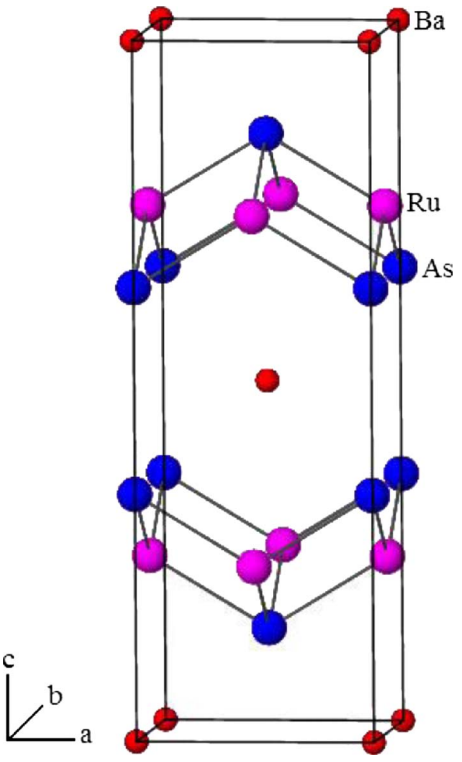

FIG. 1. (Color online) Crystal structure of $BaRu_2As_2$ with the tetragonal $ThCr_2Si_2$-type structure showing RuAs and Ba layers alternating along the c-axis.

discuss the properties of $BaRu_2As_2$ and $SrRu_2As_2$ in the context of other $ThCr_2Si_2$-type and ZrCuSiAs-type transition metal pnictides. From this comparison, it appears that a large Stoner enhancement of the conduction electron spin susceptibility is needed for high T_c in this class of materials.

II. EXPERIMENTAL DETAILS

Polycrystalline samples of $BaRu_2As_2$ and $SrRu_2As_2$ were prepared by solid state reaction techniques using elemental Ba (99.999% pure), Sr (99.99% pure), Ru (99.9999% pure), and As (99.999% pure). The stoichiometric mixtures in an Al_2O_3 crucible were sealed inside an evacuated quartz tube. At first, the elements were heated slowly up to 610 °C at a rate of 80 °C/h, kept there for 10 h, and then heated up to 850 °C and kept there for 20 h. The samples were then progressively fired at 950 and 1000 °C for 20 h, each followed by one intermediate grinding and pelletization. For the final firing at 1000 °C, the pellets were wrapped in a Ta foil before sealing in the quartz tube. All the sample handling was carried out inside a He-filled glove box. Our repeated attempts to grow crystals using Sn, Pb, and In fluxes followed by slow cooling failed.

The samples were characterized using a Rigaku Geigerflex powder x-ray diffractometer and Cu K_α radiation (λ_{av} =1.54182 Å). The powder pattern evidenced almost single phase material with a small impurity peak of about 2% and 3% relative intensity for the Ba and Sr compounds, respectively, which is suspected to arise from unreacted Ru. Unlike the Sr compound, for the Ba compound there appears another tiny impurity peak at the position expected for the strongest peak of $BaCO_3$ at $2\theta \approx 25°$ (marked by a star) which has about 1.5% relative intensity. These impurities should not measurably affect the $\chi(T)$ or $C_p(T)$ data but may have an unknown effect on the $\rho(T)$ data. Rietveld refinements of the data were carried out using the GSAS package.[25] Figure 2 shows the Rietveld refinement fit to the x-ray powder diffraction pattern for $BaRu_2As_2$. All the peaks except for the above impurity peak (see inset of Fig. 2) could be indexed and fitted based on the $ThCr_2Si_2$ structure with $I4/mmm$ space group. The goodness of the fit is 5.3% and 7.5% for the Ba and Sr compounds, respectively. The obtained lattice parameters are [a=4.152 48(8) Å, c =12.2504(3) Å] and [a=4.1713(1) Å, c=11.1845(4) Å] for the Ba and Sr compounds, respectively. These values are close to the above previously reported ones.[23] Our refined z parameters for the As atoms are 0.3527(1) for $BaRu_2As_2$ and 0.3612(2) for $SrRu_2As_2$.

The magnetization M and magnetic susceptibility $\chi(T) \equiv M/H$, where H is the applied magnetic field, were measured in the temperature T range 1.8 K$\leq T \leq$300 K on polycrystalline samples in a commercial Quantum Design superconducting quantum interference device (SQUID) magnetometer. dc resistivity $\rho(T)$ was measured using a standard four-probe technique by applying a current of 5 mA, and heat capacity $C_p(T)$ was measured on a small piece of sample with mass about 8 mg. Both $\rho(T)$ and $C_p(T)$ measurements were performed on sintered pellets using a Quantum Design Physical Property Measurement System.

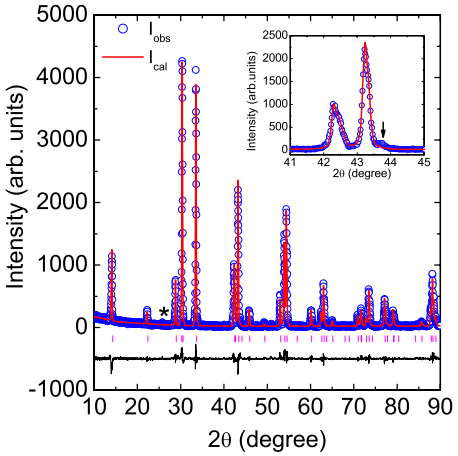

FIG. 2. (Color online) X-ray powder-diffraction pattern (open circles) at room temperature for $BaRu_2As_2$. The solid line represents the Rietveld refinement fit with the $ThCr_2Si_2$ structure and $I4/mmm$ space group. The impurity peak corresponding to $BaCO_3$ is marked by a star. Inset: small section of the x-ray powder pattern is magnified to highlight the unidentified impurity peak marked by an arrow, which might be due to unreacted Ru metal.

III. EXPERIMENTAL RESULTS AND ANALYSIS

Figure 3 shows the temperature dependence of resistivity $\rho(T)$ for $BaRu_2As_2$ and $SrRu_2As_2$. With decreasing temperature, $\rho(T)$ decreases for both compounds to a residual resistivity at 2 K of about 9.7 and 2300 $\mu\Omega$ cm for the Ba and Sr compounds, respectively. This type of temperature dependence suggests metallic behavior of the compounds. We did not observe any clear anomaly that might be associated with an SDW down to 2 K. The residual resistivity ratio ρ(310 K)/ρ(2 K) was found to be about 17 and 5 for the Ba and Sr compounds, respectively. These values are comparable to those reported for polycrystalline $(Ba,Sr)Fe_2As_2$.[15,16]

The heat capacity C_p vs T at zero field for $BaRu_2As_2$ and $SrRu_2As_2$ is shown in Fig. 4. We did not observe any clear anomaly associated with a SDW or structural transition down

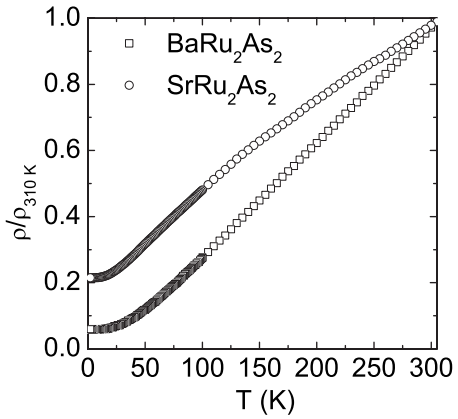

FIG. 3. Normalized dc electrical resistivity ρ versus temperature T of $BaRu_2As_2$ and $SrRu_2As_2$. The room-temperature resistivity ρ(310 K) values are 170 $\mu\Omega$ cm and 10.7 mΩ cm for $BaRu_2As_2$ and $SrRu_2As_2$, respectively. The unexpectedly large value for $SrRu_2As_2$ may arise from a high porosity of the sample.

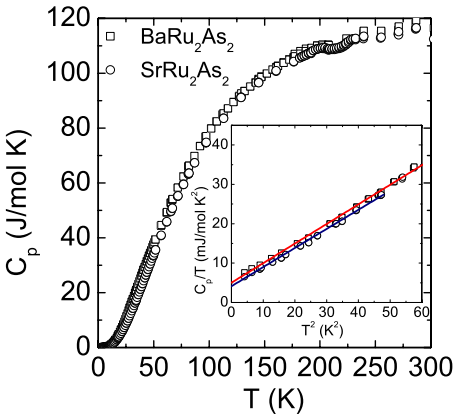

FIG. 4. (Color online) Heat capacity C_p vs temperature T for $BaRu_2As_2$ and $SrRu_2As_2$. The inset shows C_p/T vs T^2 at low temperatures and the two solid lines are the respective linear fits.

to 2 K. However, the small anomaly at about 200 K for $SrRu_2As_2$ may be a real effect in view of the cusp at the same temperature found in the measurement of $\chi(T)$ below. The value of C_p at room temperature is about 120 J/mol K which is close to the Dulong Petit lattice heat-capacity value $C_p=15R\simeq 125$ J/mol K expected for our compounds,[26] where R is the molar gas constant. As shown in the inset of Fig. 4, $C_p(T)/T$ vs T^2 is almost linear at low-T ($T<8$ K) and was fitted by the expression $C_p/T=\gamma+\beta T^2$, where γ is the Sommerfeld coefficient of electronic heat capacity and the second term accounts for the lattice contribution with coefficient β. The resultant γ and β values are [4.9(1) mJ/mol K^2 and 0.49(4) mJ/mol K^4] and [4.1(1) mJ/mol K^2 and 0.49(2) mJ/mol K^4] for the Ba and Sr compounds, respectively.

The density of states at the Fermi energy for both spin directions $N(E_F)$ can be estimated using the value of γ in the following relation,[26]

$$\gamma=\frac{\pi^2}{3}k_B^2N(E_F)(1+\lambda_{ep}), \tag{1}$$

where λ_{ep} is the electron-phonon coupling constant. As a first approximation we set $\lambda_{ep}=0$, which gives $N(E_F)=2.1(1)$ and 1.7(1) states/(eV f.u.) (f.u. stands for formula unit) for the Ba and Sr compounds, respectively. These densities of states are comparable with our previously reported value of 2.0(4) states/(eV f.u.) for $BaRh_2As_2$ estimated in the same way from heat capacity measurements.[27] In $BaRh_2As_2$ band structure calculations indicate that the maximum contribution to $N(E_F)$ comes from the Rh $4d$ states.[27] From $N(E_F)$ one can calculate the bare Pauli paramagnetic spin susceptibility of the conduction carriers χ_P using[26]

$$\chi_P=\mu_B^2N(E_F), \tag{2}$$

where μ_B is the Bohr magneton. This gives $\chi_P\simeq 6.8\times 10^{-5}$ and 5.5×10^{-5} cm^3/mol for the Ba and Sr compounds, respectively. These values are comparable to that found in $BaRh_2As_2$.[27] From the value of β one can also estimate the Debye temperature Θ_D using the expression,[26]

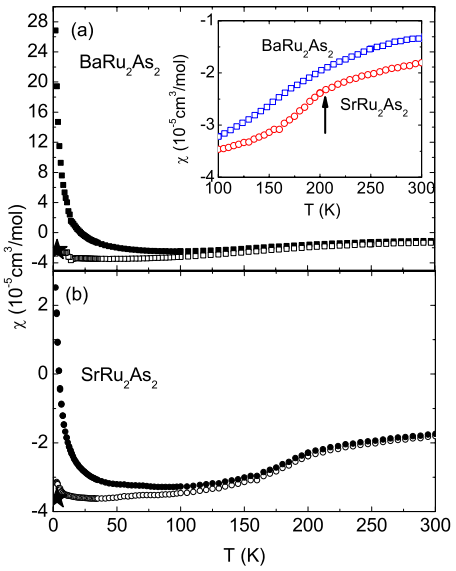

FIG. 5. (Color online) Magnetic susceptibility $\chi\equiv M/H$ of (a) $BaRu_2As_2$ and (b) $SrRu_2As_2$ versus temperature T (solid symbols) measured in an applied magnetic field $H=1$ T. The magnetization M data are corrected for the contributions from ferromagnetic impurities as determined from the $M(H)$ isotherm data in Fig. 6 (see text). The intrinsic $\chi(T)$ after correction for the additional contribution of paramagnetic impurities (see text) is also shown (open symbols). The star symbols are the χ_0 values in Eq. (4) estimated from the analysis of magnetization versus field isotherms at low temperatures. In the inset of (a) the intrinsic $\chi(T)$ data are magnified for both compounds and the arrow points to the anomaly around 200 K for $SrRu_2As_2$.

$$\Theta_D=\left(\frac{12\pi^4Rn}{5\beta}\right)^{1/3}, \tag{3}$$

where n is the number of atoms per formula unit ($n=5$ for our compounds). The above β values yield $\Theta_D=271(7)$ and 271(4) K for the Ba and Sr compounds, respectively, which are comparable to the values of ~280 (Ref. 28) and 246(3) K (Ref. 29) reported for isostructural $BaMn_2As_2$ but are larger than the value of 171(2) K reported for $BaRh_2As_2$.[27]

For both the magnetic susceptibility $\chi(T)$ and magnetization $M(H,T)$ measurements we carried out, the data were corrected for the contribution of the empty sample holder, which was not negligible. The $\chi\equiv M/H$ as a function of temperature in a field $H=1$ T is shown in Fig. 5, where the M data are corrected for the contributions from ferromagnetic impurities as determined from the $M(H)$ isotherm data in Fig. 6 below. $\chi(T)$ at high temperatures is negative and weakly temperature dependent. At low temperatures, $\chi(T)$ shows a Curielike upturn. For the Ba compound this upturn is much stronger than the Sr one. This upturn is attributed to extrinsic paramagnetic impurities and/or magnetic defects in the samples, as now discussed.

Magnetization M as a function of applied magnetic field H was measured at different temperatures. Figure 6 shows the $M(H)$ isotherms at different temperatures for both compounds measured up to $H=5.5$ T. For both compounds $M(H)$ shows a negative curvature below a field of 1 T at all

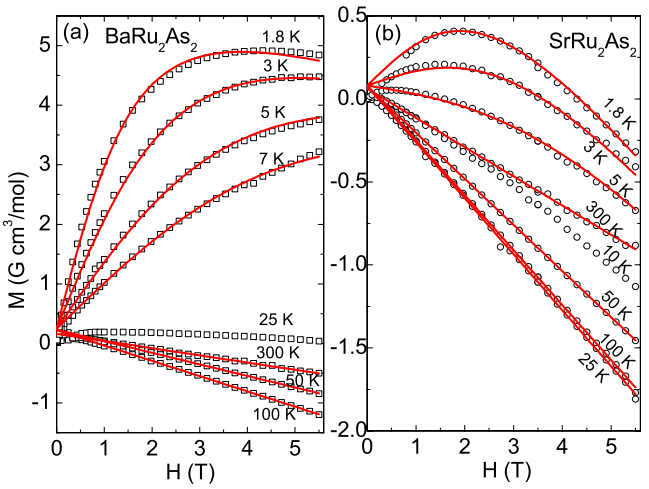

FIG. 6. (Color online) Magnetization M versus field H isotherms for (a) $BaRu_2As_2$ and (b) $SrRu_2As_2$ at different temperatures. For $SrRu_2As_2$ at 1.8 K, we were not able to collect data below 5 kOe where the sum of the signals from the sample and sample holder is nearly zero. Solid curves are the fits by Eq. (4) at 1.8, 3, 5, and 7 K for the Ba compound, and at 1.8, 3, and 5 K for the Sr compound. The straight lines are fits to the data for $H \geq 1$ T at ≥ 50 K for the Ba compound and at ≥ 25 K for the Sr compound by $M = M_s + \chi H$.

temperatures due to the saturation of ferromagnetic impurities. To estimate the saturation magnetization M_s of the ferromagnetic impurities, we fitted magnetization isotherms at high temperatures (≥ 50 K for $BaRu_2As_2$ and ≥ 25 K for $SrRu_2As_2$) to a straight line ($M_s + \chi H$) above 1 T, as shown by the straight-line fits in Fig. 6. The M_s was found to be nearly independent of T with values of about 0.247 and 0.081 G cm^3/mol at low temperatures for the Ba and Sr compounds, respectively. The near constant values of M_s versus temperature indicate that the Curie temperature(s) of the ferromagnetic impurities are significantly above 300 K. The low-T M_s values correspond to the contributions of the equivalent of 20 and 6.6 molar ppm of Fe metal impurities to the M of the Ba and Sr compounds, respectively. The plotted magnetic susceptibilities at $H = 1$ T as given above by the filled symbols in Fig. 5 are given by $\chi(T) = [M(T) - M_s(T)]/H$.

For a quantitative estimation of the paramagnetic impurity contribution giving rise to the upturns in the susceptibilities at low temperatures, we fitted our $M(H)$ data for 1 T $\leq H \leq 5.5$ T at 1.8, 3, 5, and 7 K for the Ba compound, and 1.8, 3, and 5 K for the Sr compound simultaneously by the equation

$$M = M_s + \chi_0 H + f_{imp} N_A g_{imp} \mu_B S_{imp} B_{S_{imp}}(x), \qquad (4)$$

where M_s is the above-determined low-temperature ferromagnetic impurity saturation value, f_{imp} is the molar fraction of the impurities, N_A is Avogadro's number, g_{imp} is the impurity g-factor, S_{imp} is the impurity spin, $B_{S_{imp}}(x)$ is the Brillouin function,[26] and χ_0 is the intrinsic susceptibility of the sample. The modified argument of the Brillouin function is $x = g_{imp}\mu_B S_{imp} H/[k_B(T - \theta_{imp})]$, where θ_{imp} is the Weiss temperature due to impurity interactions. To reduce the number of fitting parameters, the impurity g-factor was set to $g_{imp} = 2$. The obtained fitting parameters (χ_0, f_{imp}, S_{imp}, and θ_{imp}) are $[-2.3(1) \times 10^{-5}$ cm^3/mol, 0.0284(3) mol %, 1.85(3), and $-0.46(6)$ K] and $[-3.62(6) \times 10^{-5}$ cm^3/mol, 0.0092(1) mol %, 1.62(4), and $-1.2(1)$ K] for the Ba and Sr compounds, respectively. The Curie constant C_{imp} of the paramagnetic impurities was calculated using $C_{imp} = f_{imp} N_A g_{imp}^2 \mu_B^2 S_{imp}(S_{imp}+1)/3k_B$, which yields $C_{imp} \approx 0.754 \times 10^{-3}$ cm^3 K/mol and 0.195×10^{-3} cm^3 K/mol for the Ba and Sr compounds, respectively. Our intrinsic $\chi(T)$ data that are corrected for both the ferromagnetic impurity and paramagnetic impurity contributions are shown in Fig. 5 as open symbols. The low-T χ_0 values obtained from the magnetization isotherm analysis are also plotted as filled stars in Fig. 5 and are, of course, in agreement with the intrinsic $\chi(T)$ data.

From the open symbols in Fig. 5, the intrinsic susceptibilities of $BaRu_2As_2$ and $SrRu_2As_2$ are diamagnetic over the whole T range, becoming somewhat more negative with decreasing T. A diamagnetic susceptibility is not unprecedented for a transition metal compound, as seen, e.g., for $LaRu_2P_2$ (Ref. 23), and OsB_2 and RuB_2.[30] As shown in the inset of Fig. 5, the intrinsic $\chi(T)$ of $SrRu_2As_2$ shows a (reproducible) small cusp around 200 K in contrast to the smooth behavior observed in $BaRu_2As_2$. This cusp for $SrRu_2As_2$ is qualitatively similar to the cusp seen for 1111 and 122 parent compounds, and attributed to structural/SDW transitions.[4,13–20] The temperature of the cusp is similar to the temperature of the small anomaly in $C_p(T)$ in Fig. 4 so the latter anomaly may not be an artifact.

IV. DISCUSSION

The intrinsic $\chi(T)$ of a metal can be written as $\chi = \chi_D + \chi_{VV} + \chi_P$, where χ_D includes the orbital diamagnetism of the core electrons (χ_{core}) and the orbital Landau diamagnetism (χ_L) of the conduction electrons, χ_{VV} is the orbital Van Vleck paramagnetism, and χ_P is the Pauli-spin paramagnetism of the conduction electrons. For an extended system it is difficult to calculate χ_D due to intercell currents. Nevertheless one can roughly estimate the χ_{core} of the compounds assuming an ionic picture, where (Ba or Sr), Ru, and As are in 2+, 2+, and 3− oxidation states, respectively.[31] This estimate will give the upper limit to the χ_D. In this way χ_{core} was calculated to be -1.6×10^{-4} and -1.43×10^{-4} cm^3/mol for the Ba and Sr compounds, respectively. Since χ_P is positive, when added to the negative χ_{core}, the result is a reduced positive value or even a negative value of χ. Using the χ_P values obtained from the above heat capacity data analysis, the sum of χ_{core} and χ_P is $\approx -9 \times 10^{-5}$ cm^3/mol for both compounds. This value is somewhat more negative than the intrinsic values in Fig. 5, suggesting that the Van Vleck paramagnetic orbital susceptibility χ_{VV} and/or Stoner enhancement of χ_P are not negligible in these compounds. This value is also of the same order of magnitude as has been estimated for $BaRh_2As_2$.[27]

In the following discussion we relate the properties of the $(Sr,Ba)Ru_2As_2$ compounds with those of other $ThCr_2Si_2$-type and ZrCuSiAs-type pnictides, and consider

their superconducting transition temperature T_c or lack thereof. Lee and co-workers[32,33] and Zhao *et al.*[34] found an interesting correlation for a wide range of parent compounds $Ba(Fe,Ni)_2(P,As)_2$ and *Ln*(Fe,Ni)(P,As)O, where *Ln* is a rare-earth element: the highest T_c occurred for the doped materials in which the respective $FeAs_4$ tetrahedra were least distorted.[32–34] Within a MPn_4 tetrahedron, where *M* is the transition metal and *Pn*=P or As, there is a twofold *Pn*-*M*-*Pn* bond angle where the two *Pn* atoms are on the same side of the *M* atom layer along the *c*-axis, and there is a fourfold *Pn*-*M*-*Pn* bond angle where the two *Pn* atoms are on opposite sides of the *M* layer (see Fig. 1). The angle plotted in Refs. 32 and 33 is the twofold *Pn*-*M*-*Pn* bond angle.

We have calculated the twofold As-Ru-As bond angles from our structural data for the $(Sr,Ba)Ru_2As_2$ compounds and also for the As-Rh-As bond angle for $BaRh_2As_2$.[27] For the body-centered-tetragonal $BaFe_2As_2$-type and the primitive tetragonal LaFeAsO-type structures, the twofold and fourfold As-Fe-As bond angles are given by

$$\theta_2 = \arccos\left[\frac{-\frac{a^2}{4} + (z-\alpha)^2 c^2}{r^2}\right] \quad \text{(twofold)},$$

$$\theta_4 = \arccos\left[\frac{-(z-\alpha)^2 c^2}{r^2}\right] \quad \text{(fourfold)}, \tag{5}$$

where

$$r^2 = \frac{a^2}{4} + (z-\alpha)^2 c^2,$$

and $\alpha=1/4$ for the $BaFe_2As_2$-type structure and $\alpha=1/2$ for the LaFeAsO-type structure. Here *a* and *c* are the lattice parameters, *z* is the *z*-axis position parameter of the As atom in the respective structure ($z\approx0.35$ in $BaFe_2As_2$ and $z\approx0.65$ in LaFeAsO), and *r* is the nearest-neighbor Fe-As distance within an Fe-centered $FeAs_4$ tetrahedron (all four Fe-As nearest-neighbor distances are the same in each of the two structures). The Fe atoms in both structures form a square lattice where the fourfold nearest-neighbor Fe-Fe distance in both structures is $d_{\text{Fe-Fe}}=a/\sqrt{2}$.

Using Eq. (5), we find $\theta_2=117.6°$, 118.4°, and 112.2° for $BaRu_2As_2$, $SrRu_2As_2$, and $BaRh_2As_2$, respectively. These bond angles for the $(Ba,Sr)Ru_2As_2$ compounds are significantly larger than the above optimum value of ≈109.47° for the Fe(P,As)-based materials and therefore the low T_c's <1.8 K for the $(Ba,Sr)Ru_2As_2$ compounds are consistent with this overall behavior. On the other hand, $BaRh_2As_2$ stands out as an exception: it has the same θ_2 as the high-temperature superconducting LaFeAsO-based and CeFeAsO-based compounds with $T_c=28-40$ K (Refs. 32 and 34) but is not superconducting. Therefore, at least one additional characteristic of the materials must be controlling T_c. As will be discussed in detail elsewhere,[35] the bare nonmagnetic band-structure density of states at the Fermi energy $N(E_F)$ is not correlated with T_c. For example, the calculated $N(E_F)$ for nonsuperconducting $BaRh_2As_2$ and that of superconducting $LaFeAsO_{0.9}F_{0.1}$ with $T_c=27$ K are the same. The values are 1.76 (Ref. 27) and 1.28–2.01 states/(eV *M* atom) (Refs. 36 and 37), respectively, for both spin directions.

On the other hand, $\chi(300\ \text{K})$ is large for all FeAs-based compounds with high T_c, suggesting that Stoner enhancement of the susceptibility may be relevant to the superconducting mechanism.[35] Again using the same examples as above, for $BaRh_2As_2$ one finds a powder averaged $\bar{\chi}(300\ \text{K})=0.18\times10^{-4}$ cm^3/(mol Rh),[27] whereas for $LaFeAsO_{0.9}F_{0.1}$ one obtains $\bar{\chi}(300\ \text{K})=3.3\times10^{-4}$ cm^3/(mol Fe),[38] which is a factor of 18 larger. For $LaFeAsO_{0.9}F_{0.1}$, the above $N(E_F)$ range predicts a bare Pauli conduction electron spin susceptibility of $0.41-0.65\times10^{-4}$ cm^3/(mol Fe), suggesting a Stoner enhancement by a factor of 5 to 8. However, accurate estimates of the enhancement factor require that orbital contributions to χ must be corrected for.[35]

V. CONCLUSION

We have synthesized and investigated the physical properties of $ThCr_2Si_2$-type polycrystalline $BaRu_2As_2$ and $SrRu_2As_2$ compounds. Both compounds were found to be metallic in character. Unlike other similar *isoelectronic* compounds $(Ca,Sr,Ba)Fe_2As_2$, $BaRu_2As_2$ shows no signature of a spin density wave or a structural transition from $\rho(T)$, $\chi(T)$, or $C_p(T)$ measurements down to 1.8 K. However, a clear cusp in $\chi(T)$ and a hint of one in $C_p(T)$ was found at ~200 K for $SrRu_2As_2$, which may be indicative of a structural and/or magnetic transition.

From analysis of our $C_p(T)$ data, the density of states at the Fermi energy $N(E_F)$ for $(Ba,Sr)Ru_2As_2$ was estimated to be ~1 state/(eV Ru atom) for both spin directions and is comparable to that per Rh atom in $BaRh_2As_2$. The small and negative values of $\chi(T)$ for both $BaRu_2As_2$ and $SrRu_2As_2$ indicate small or negligible Stoner enhancement of the conduction electron spin susceptibility. A comparison of $N(E_F)$ with that of $BaRh_2As_2$ suggests that the maximum contribution to $N(E_F)$ comes from the Ru 4*d* states. It would be interesting to study the effect of doping of $SrRu_2As_2$ in view of the occurrence of superconductivity in $Ba_{1-x}K_xFe_2As_2$, $Sr_{1-x}K_xFe_2As_2$, and $BaFe_{2-x}Ru_xAs_2$.[7,10,39] Finally, a comparison of the properties of $(Ba,Sr)Ru_2As_2$ and $BaRh_2As_2$ with those of the FeAs-based materials indicates that $N(E_F)$ for these nonsuperconducting Ru and Rh arsenides is about the same as for FeAs-based compounds with high T_c.[35] A distinguishing feature of the high T_c FeAs-based materials is their large χ values that evidently reflect significant Stoner enhancement of the conduction electron spin susceptibility[35] as has been pointed out before.[40–42] Thus it seems possible that the mechanisms for the Stoner enhancement and for the high T_c in the FeAs-based materials may be closely related.

ACKNOWLEDGMENT

Work at the Ames Laboratory was supported by the Department of Energy–Basic Energy Sciences under Contract No. DE-AC02-07CH11358.

[1] Y. Kamihara, T. Watanabe, M. Hirano, and H. Hosono, J. Am. Chem. Soc. **130**, 3296 (2008).
[2] Z.-A. Ren, W. Lu, J. Yang, W. Yi, X. L. Shen, C. Zheng, G. C. Che, X. L. Dong, L. L. Sun, F. Zhou, and Z. X. Zhao, Chin. Phys. Lett. **25**, 2215 (2008).
[3] X. H. Chen, T. Wu, G. Wu, R. H. Liu, H. Chen, and D. F. Fang, Nature (London) **453**, 761 (2008).
[4] G. F. Chen, Z. Li, D. Wu, G. Li, W. Z. Hu, J. Dong, P. Zheng, J. L. Luo, and N. L. Wang, Phys. Rev. Lett. **100**, 247002 (2008).
[5] Z.-A. Ren, J. Yang, W. Lu, W. Yi, X.-L. Shen, Z.-C. Li, G.-C. Che, X.-L. Dong, L.-L. Sun, F. Zhou, and Z.-X. Zhao, Europhys. Lett. **82**, 57002 (2008).
[6] P. Quebe, L. Terbuchte, and W. Jeitschko, J. Alloys Compd. **302**, 70 (2000).
[7] M. Rotter, M. Tegel, and D. Johrendt, Phys. Rev. Lett. **101**, 107006 (2008).
[8] G. F. Chen, Z. Li, G. Li, W.-Z. Hu, J. Dong, J. Zhou, X.-D. Zhang, P. Zheng, N.-L. Wang, and J.-L. Luo, Chin. Phys. Lett. **25**, 3403 (2008).
[9] H. S. Jeevan, Z. Hossain, D. Kasinathan, H. Rosner, C. Geibel, and P. Gegenwart, Phys. Rev. B **78**, 092406 (2008).
[10] K. Sasmal, B. Lv, B. Lorenz, A. M. Guloy, F. Chen, Y.-Y. Xue, and C. W. Chu, Phys. Rev. Lett. **101**, 107007 (2008).
[11] G. Wu, H. Chen, Y. L. Xie, Y. J. Yan, R. H. Liu, X. F. Wang, J. J. Ying, and X. H. Chen, J. Phys.: Condens. Matter **20**, 422201 (2008).
[12] M. Pfisterer and G. Nagorsen, Z. Naturforsch. B **35B**, 703 (1980).
[13] J. Dong, H. J. Zhang, G. Xu, Z. Li, G. Li, W. Z. Hu, D. Wu, G. F. Chen, X. Dai, J. L. Luo, Z. Fang, and N. L. Wang, Europhys. Lett. **83**, 27006 (2008).
[14] H.-H. Klauss, H. Luetkens, R. Klingeler, C. Hess, F. J. Litterst, M. Kraken, M. M. Korshunov, I. Eremin, S.-L. Drechsler, R. Khasanov, A. Amato, J. Hamann-Borrero, N. Leps, A. Kondrat, G. Behr, J. Werner, and B. Büchner, Phys. Rev. Lett. **101**, 077005 (2008).
[15] M. Rotter, M. Tegel, D. Johrendt, I. Schellenberg, W. Hermes, and R. Pöttgen, Phys. Rev. B **78**, 020503(R) (2008).
[16] C. Krellner, N. Caroca-Canales, A. Jesche, H. Rosner, A. Ormeci, and C. Geibel, Phys. Rev. B **78**, 100504(R) (2008).
[17] N. Ni, S. L. Bud'ko, A. Kreyssig, S. Nandi, G. E. Rustan, A. I. Goldman, S. Gupta, J. D. Corbett, A. Kracher, and P. C. Canfield, Phys. Rev. B **78**, 014507 (2008).
[18] J.-Q. Yan, A. Kreyssig, S. Nandi, N. Ni, S. L. Budko, A. Kracher, R. J. McQueeney, R. W. McCallum, T. A. Lograsso, A. I. Goldman, and P. C. Canfield, Phys. Rev. B **78**, 024516 (2008).
[19] Z. Ren, Z. Zhu, S. Jiang, X. Xu, Q. Tao, C. Wang, C. Feng, G. Cao, and Z. Xu, Phys. Rev. B **78**, 052501 (2008).
[20] H. S. Jeevan, Z. Hossain, D. Kasinathan, H. Rosner, C. Geibel, and P. Gegenwart, Phys. Rev. B **78**, 052502 (2008).
[21] T. Mine, H. Yanagi, T. Kamiya, Y. Kamihara, M. Hirano, and H. Hosono, Solid State Commun. **147**, 111 (2008).
[22] F. Ronning, N. Kurita, E. D. Bauer, B. L. Scott, T. Park, T. Klimczuk, R. Movshovich, and J. D. Thompson, J. Phys.: Condens. Matter **20**, 342203 (2008).
[23] W. Jeitschko, R. Glaum, and L. Boonk, J. Solid State Chem. **69**, 93 (1987).
[24] G. Wenski and A. Mewis, Z. Naturforsch. B **41B**, 38 (1986).
[25] A. C. Larson and R. B. Von Dreele, Los Alamos National Laboratory Report No. LAUR 86–748, 2000 (unpublished); B. H. Toby, J. Appl. Crystallogr. **34**, 210 (2001).
[26] C. Kittel, *Introduction to Solid State Physics*, 4th ed. (Wiley, New York, 1966).
[27] Y. Singh, Y. Lee, S. Nandi, A. Kreyssig, A. Ellern, S. Das, R. Nath, B. N. Harmon, A. I. Goldman, and D. C. Johnston, Phys. Rev. B **78**, 104512 (2008).
[28] J. An, A. S. Sefat, D. J. Singh, M. H. Du, and D. Mandrus, Phys. Rev. B **79**, 075120 (2009).
[29] Y. Singh, A. Ellern, and D. C. Johnston, Phys. Rev. B **79**, 094519 (2009).
[30] Y. Singh, A. Niazi, M. D. Vannette, R. Prozorov, and D. C. Johnston, Phys. Rev. B **76**, 214510 (2007).
[31] P. W. Selwood, *Magnetochemistry*, 2nd ed. (Interscience, New York, 1956), p. 78.
[32] C.-H. Lee, A. Iyo, H. Eisaki, H. Kito, M. T. Fernandez-Diaz, T. Ito, K. Kihou, H. Matsuhata, M. Braden, and K. Yamada, J. Phys. Soc. Jpn. Suppl. C **77**, 44 (2008).
[33] C.-H. Lee, A. Iyo, H. Eisaki, H. Kito, M. T. Fernandez-Diaz, R. Kumai, K. Miyazawa, K. Kihou, H. Matsuhata, M. Braden, and K. Yamada, J. Phys. Soc. Jpn. **77**, 083704 (2008).
[34] J. Zhao, Q. Huang, C. de la Cruz, S. Li, J. W. Lynn, Y. Chen, M. A. Green, G. F. Chen, G. Li, Z. Li, J. L. Luo, N. L. Wang, and P. Dai, Nature Mater. **7**, 953 (2008).
[35] D. C. Johnston *et al.* (unpublished).
[36] I. I. Mazin, D. J. Singh, M. D. Johannes, and M. H. Du, Phys. Rev. Lett. **101**, 057003 (2008).
[37] G. Wang, Y. Qian, G. Xu, X. Dai, and Z. Fang, arXiv:0903.1385 (unpublished).
[38] R. Klingeler, N. Leps, I. Hellmann, A. Popa, C. Hess, A. Kondrat, J. Hamann-Borrero, G. Behr, V. Kataev, and B. Büchner, arXiv:0808.0708 (unpublished); A. Kondrat, J. E. Hamann-Borrero, N. Leps, M. Kosmala, O. Schumann, J. Werner, G. Behr, M. Braden, R. Klingeler, B. Büchner, and C. Hess, arXiv:0811.4436 (unpublished); R. Klingeler, private communication.
[39] S. Paulraj, S. Sharma, A. Bharathi, A. T. Satya, S. Chandra, Y. Hariharan, and C. S. Sundar, arXiv:0902.2728 (unpublished).
[40] D. J. Singh and M.-H. Du, Phys. Rev. Lett. **100**, 237003 (2008); D. J. Singh, arXiv:0901.2149 (unpublished).
[41] Y. Kohama, Y. Kamihara, M. Hirano, H. Kawaji, T. Atake, and H. Hosono, Phys. Rev. B **78**, 020512(R) (2008).
[42] K. Haule and G. Kotliar, New J. Phys. **11**, 025021 (2009).